DOI: 10.1002/anie.201408969

Photoluminescence

Nanoribbon-Structured Organo Zinc Phosphite Polymorphs with White-Light Photoluminescence**

*Hui-Lin Huang and Sue-Lein Wang**

Abstract: *The first neutral organo zinc phosphites composed of 2.8 nm-wide ribbons were obtained in pure phases and exhibit near-white-light photoluminescence (PL). By using the "mesitylene strategy", interesting polymorphism in the system of NTHU-14 was discovered. The S-shaped ribbons are arranged into R and L arrays, resulting in RLR and RRR stacking for two polymorphs. π–π interactions exist within each array and hydrogen bonding between adjacent arrays. Besides a common ligand-based emission band at 410 nm, the PL curves of polymorphs 14-α and 14-β are distinctly different: 14-α gave a defect-based emission at 565 nm, whereas 14-β primarily shows a π-excimer-based emission at 535 nm. Electron paramagnetic resonance (EPR) data disclosed that radical species exist in the reaction and that the two phases were growing from different environments. Based on these results, the origin of the 565 nm band can be ascribed to lattice defects, and one possible cause of 14-β not showing noticeable yellow emission is identified.*

Crystalline materials with open-framework structures have shown a great variety of topology, interesting new properties, and multifaceted functionality, and may lead to a better understanding of structure–property relationships as well as to potential applications, particularly energy-related ones.[1] In the past two decades, these materials have been progressively developed from those with inorganic frameworks of aluminosilicates, germanium oxides, and phosphorus-based metal phosphates/phosphites (MPOs)[2,3] to those with organic–inorganic hybrid structures such as coordination polymers and metal–organic frameworks (MOFs).[4] Strategically, the successful formation of structures with either pure inorganic or hybrid frameworks usually requires the use of organic chemicals as structure-directing reagents or templates. Recently, a major breakthrough in mesoporous inorganic frameworks in the MPO system has been achieved with the 56-, 64-, and 72-membered-ring channel structures of NTHU-13, in which the inorganic mesoporous channel is firstly shown to possess a completely crystalline ordered pore-wall structure.[5] In addition to the usual organic amine templates, the organic reagent mesitylene (1,3,5-trimethylbenzene, TMB) was introduced for channel expansion. TMB is well-known as a swelling reagent in the synthesis of amorphous mesoporous silica,[6] but until the synthesis of NTHU-13 it has not been used to produce single crystals. It should be of great interest to further expand the use of such reagents for the exploration of more innovative crystalline solids.

In this work, we employed TMB in an organic–inorganic hybrid system to study its influence on the formation of a novel organo zinc phosphite compound. Beyond its conventional roles, TMB turned out to be a key factor in producing a polymorphic phase and introducing different optical properties. Polymorphic solids are interesting and valuable, because they possess identical chemical compositions but nonidentical structures; thereby, distinct properties and functions can be extracted from the same chemical systems.[7] For example, zeolite beta has two polymorphs A and B. Polymorph A has a chiral framework and can promote enantioselective catalysis, whereas the centrosymmetric polymorph B cannot.[8] Other examples are the polymorphs of interpenetration MOFs, in which open or catenated channels can lead to contrasting gas sorption properties.[9] However, compared with the more often encountered isomorphic phases (similar in structure but different in chemical composition),[10] true polymorphic phases are less explored and difficult to isolate, particularly those with open-framework structures. In this study, we show that the "mesitylene strategy" leads to pure-phase polymorph formation (Scheme 1).

In our previous work, we have prepared metal-activator-free MPO structures with intriguing white-light photoluminescence (PL), in which M = Zn, Ga, and Sn.[3,11] Most of

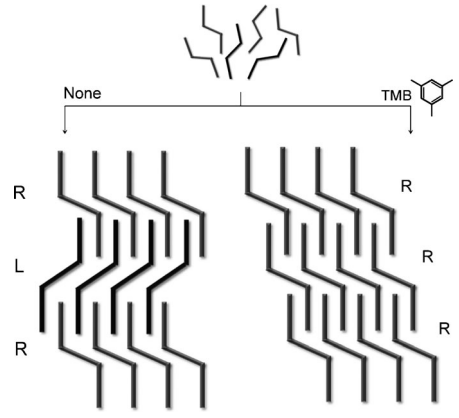

Scheme 1. Two polymorphic phases of NTHU-14: 14-α (left) and 14-β (right), showing different stacking modes of ribbon arrays under the preparation with or without TMB in reaction.

[*] Dr. H.-L. Huang, Prof. S.-L. Wang
Department of Chemistry, National Tsing Hua University
No. 101, Section 2, Kuang-Fu Road, Hsinchu 30013 (Taiwan)
E-mail: slwang@mx.nthu.edu.tw

[**] This research was supported by the Ministry of Science and Technology (MOST 103-2113-M-007-003-MY3) and the National Synchrotron Radiation Research Center of Taiwan.

Supporting information for this article is available on the WWW under http://dx.doi.org/10.1002/anie.201408969.

them contain 4,4′-trimethylenedipyridine (TMDP, $C_{13}H_{14}N_2$) as a common organic template. In an attempt to generate new luminescent metal phosphites, we combined the metal sources of tin and zinc with TMDP and phosphorous acid in one-pot hydrothermal reactions and successfully prepared a novel white-light emitting organo zinc phosphite, $[Zn_2(H_2O)(HPO_3)(C_2O_4)(tmdp)]$ (NTHU-14). A preliminary X-ray diffraction analysis showed that the structure contains merely arrays of neutral ribbons. The intuitive intention to increase ribbon spacing led us to introduce TMB to the mixture of reactants. Surprisingly, a polymorph of NTHU-14 was thus generated. The two polymorphic phases, hereafter designated as 14-α and 14-β are both acicular transparent crystals but in different crystal systems, and could be individually prepared in pure phase with yields of 60% and 40%, respectively (based on Zn). Presumably, the presence of TMB, having a nonpolar character and a higher boiling point, may exert certain synergistic effects on entropy and pressure so that the reaction system favors the formation of 14-β, which has a lower symmetry and higher density (see below) than 14-α. Single-crystal structure analyses were performed to determine the structures and chemical formulas.[12] The organic and water contents were also corroborated by elemental and thermogravimetric (TG) analysis (see the Supporting Information).

The hybrid structures of both polymorphs exclusively consist of S-shaped ribbons with a width of 2.8 nm (Figure 1). Although the space groups are different ($P2_1/c$ for 14-α and $P\bar{1}$ for 14-β), their asymmetric unit contents are similar, consisting of two unique Zn sites (one ZnO_3N tetrahedron and one $ZnO_4(H_2O)N$ octahedron) and three unique ligands (HPO_3, oxalate, and TMDP; Figure S1). The ribbons are all alike, neutral, and centrosymmetric, and each is formed of two linear zincoxalate infinite chains of $_\infty[Zn(H_2O)(C_2O_4)]$ apart by ca. 28 Å, one four-ring zinc phosphite infinite chain of $_\infty[Zn(HPO_3)]$, and TMDP molecules bridging the zinc oxalate and zinc phosphite chains. The middle zinc phosphite chains (residing on inversion centers) show less usual outward metal sites of Zn (for TMDP coordination), whose connectivity can be compared with that occurring in NTHU-13[5] (Figure S2). The outer edges of the nanometer-wide ribbon are water ligands, 5.34 Å apart along the edge, because they are sticking out of the zinc oxalate chains. It endows hydrophilic character to all neutral ribbon edges.

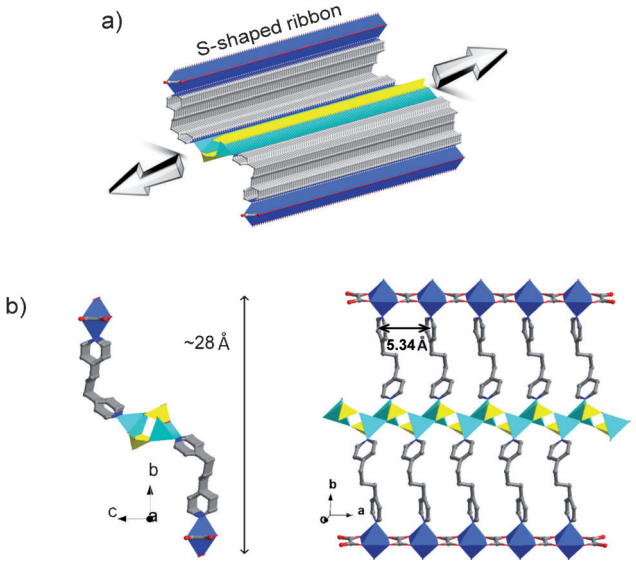

Figure 1. Plots of the neutral ribbon in NTHU-14: a) section of the S-shaped 1-D ribbon, b) views of the ribbon along the *a* and *c* axis, respectively, showing the width of the ribbon, the two zinc oxalate infinite chains forming the two edges of a ribbon, the central zinc phosphite 4-ring chain, and the TMDP ligand molecules, each bridging one edge and one middle chain. Tetrahedra of Zn in cyan, P in yellow, and octahedra of Zn in blue.

The two polymorph structures are different, primarily in the ribbon stacking modes. In 14-α, S-shaped ribbons are observed to arrange into right-bent (R) and left-bent (L) arrays (Figure 2), and the R and L arrays are 2_1 symmetry-related. In 14-β, all ribbons are in R arrays due to lower symmetry. The ribbon arrays are stacked in the RLR mode for 14-α and RRR for 14-β. Despite different stacking modes, the two polymorphic structures are nearly identical in terms of intra- and interribbon-bonding interactions, for example, 1) the TMDP ligand molecules are all in the *trans–gauche* conformation with an intramolecular N···N distance of 9.019 Å;[13] 2) no π–π interaction between intra-ribbon TMDP ligands is present, because the pyridyl rings of adjacent ligands are distant (plane-to-plane distance 5.34 Å; Figure 1); 3) TMDP π–π pairs solely occur within individual ribbon arrays, the π–π distance is 3.40 Å, the pyridyl ring centroid–centroid distance is 4.28 Å and the angle is 31.4°; and 4) hydrogen bonds exist between different ribbon arrays. The nearest contact between ribbons was found to occur between phosphite oxygen atoms belonging to one array and water oxygen atoms belonging to an adjacent array with an O···O distance of 2.77 Å (Figure 2).

TG analyses showed that removal of the coordination water molecules began at ca. 100 °C for both polymorphs 14-α and 14-β, and water ligands could be completely removed at ca. 250 °C (Figure S3). Variable-temperature powder X-ray diffraction measurements showed that the structure of 14-α is stable up to 200 °C, whereas 14-β is stable up to 250 °C (Figure S5). What is the reason for the reduced thermal stability of 14-α compared to that of 14-β? Although no significant differences were detected in any bonding interactions, we found a 0.4% difference in density between the two polymorphs. The less dense 14-α with RLR-stacked ribbons is thus slightly less rigid than the RRR-stacked 14-β. Nonetheless, from the results of TG and diffraction measurements, it may be concluded that the two neutral frameworks can be sustained even under the loss of some water molecules from the partial octahedral zinc centers. Thereby, open metal sites can be generated by heating below 200 °C for 14-α and below 250 °C for 14-β.

Both 14-α and 14-β were found to display near-white light under excitation with 320 nm UV light. Their PL emission curves are very broad and most likely involve many luminescent centers. As shown in Figure 3, the two polymorph PL emission spectra are distinctly different. In the one of 14-α two maxima can be observed, which are located at ca. 410 nm and 565 nm. The combination of these two bands

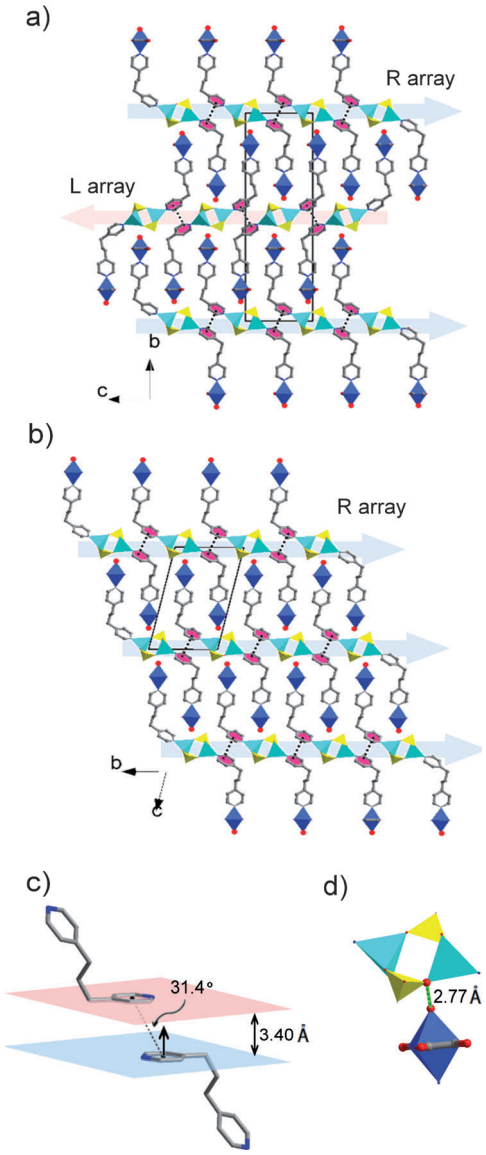

Figure 2. Structure plots of NTHU-14: a) 14-α with the ribbon arrays stacked in RLR mode; b) 14-β with the ribbon arrays stacked in RRR mode; in both (a) and (b) the adjacent TMDP ligands within an array form π–π pairs (in red); c) a closer look of the π–π pair showing the parallel planes at a distance of 3.40 Å and the ring displacement of 31.4°; and d) the nearest contact between adjacent ribbons. Tetrahedra of Zn in cyan, P in yellow, and octahedra of Zn in blue.

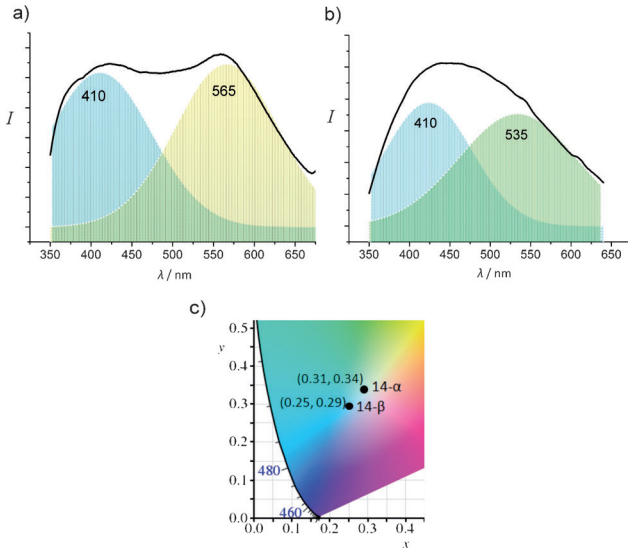

Figure 3. PL spectra and CIE chromaticity diagram showing a) the emission curve of 14-α showing two maxima at ca. 410 nm and 565 nm; b) the broad emission curve of 14-β with two embedded bands located at ca. 410 nm and 535 nm; and c) CIE coordinates indicating that the emission of 14-α is closer to white than that of 14-β.

results in near pure white light (CIE coordinates: (0.31, 0.34) with quantum efficiency (QE) of 10%). In the spectrum of 14-β one broad band is observed, which corresponds to cool-white light (CIE coordinates: (0.25, 0.29) with QE ~8%). However, in the asymmetric band two major emissions at ca. 410 nm and 535 nm were identified. The 410 nm band observed in both polymorphs can be attributed to the ligand-based emission of TMDP molecules (Figure S6). The 535 nm band, which was found in 14-β but could not be successfully isolated in 14-α, is assumed to be an excimer-based emission from aforementioned π–π pairs of TMDP.[14] The major difference in the two PL spectra evidently lies in the longer wavelength region. Based on our prior experience with those yellow-emitting MPOs,[3] the 565 nm band of the 14-α polymorph could be related to emission centers other than the π-excimers. We also found that the emission maximum from a heat-treated sample of 14-α was blue-shifted (Figure S7), showing some resemblance to defect-related PL luminescence occurring in earlier MPOs,[3,15] which had all given unanticipated EPR signals. Accordingly, we performed EPR measurements on both solid samples of the 14-α polymorph. It was not surprising that an EPR signal was observed (Figure S8). These results indicate that the 565 nm band of 14-α might originate from certain types of lattice defects occurring in MPO lattices.

We further explored the reason for the absence of a recognizable band at 565 nm in polymorph 14-β. Due to the fact that all differences between the two polymorphs result from the presence or absence of TMB in their generation, we decided to investigate the filtrates, in which the crystals of 14-α and 14-β were obtained, by EPR spectroscopy. The filtrate of 14-β was EPR-silent, whereas that of 14-α did show a signal corresponding to radical species (Figure S9). From these results, three conclusions can be drawn about the chemistry involved in our mild hydrothermal reactions: firstly, the conducted reactions lead to the generation of radical species, which are presumed to form on the aromatic amine by electron uptake; secondly, the radicals could be scavenged by using TMB, a hydroxyl radical scavenger;[16] and thirdly, crystals growing in the presence of radicals develop more lattice defects like it was observed for 14-α compared to 14-β. As a consequence, 14-β did not show a noticeable yellow emission like 14-α.

In conclusion, we have generated an innovative white-light luminescent system of organo zinc phosphites, NTHU-14, by employing organic reagents in mild hydrothermal

reactions. We have successfully demonstrated the versatile use of mesitylene/TMB for the preparation of crystalline materials, apart from its known use for the generation of noncrystalline or partially crystalline mesoporous materials. TMB is not only related to the formation of a polymorphic phase, leading to interesting nanoribbon-structured frameworks, but more importantly it leads to new results regarding the presence and elimination of radical species[17] in hydrothermal reactions that were not known before. The "mesitylene strategy" is anticipated to result in profound effects besides polymorphism and the optical properties discovered in NTHU-14. Further investigations on related systems are in progress.

Experimental Section

A pure phase of transparent crystals of 14-α was obtained by heating a mixture of zinc lactate, tin oxalate, phosphorous acid, 4,4′-trimethylenedipyridine ($C_{13}H_{14}N_2$), deionized water, ethanol, and hydrofluoric acid with absolute molar amount in the ratio 0.5:0.5:3:2:277:17:2.3 in a 23 mL Teflon-lined acid digestion bomb at 150 °C for 48 h. By including an extra 1 mL of mesitylene (1,3,5-trimethylbenzene) in the above reaction, acicular-shaped crystals of 14-β were obtained in pure phase as well. The yields (based on Zn) were 60 % and 40 % for 14-α and 14-β, respectively.

CCDC 1022642 and CCDC 1022643 contain the supplementary crystallographic data for 14-α and 14-β, respectively. These data can be obtained free of charge from The Cambridge Crystallographic Data Centre via www.ccdc.cam.ac.uk/data_request/cif.

Received: September 10, 2014
Revised: November 13, 2014
Published online: December 2, 2014

Keywords: hydrothermal synthesis · hybrid composites · polymorphism · white-light photoluminescence · zinc phosphite

[1] a) J. L. C. Rowsell, O. M. Yaghi, *Microporous Mesoporous Mater.* **2004**, *73*, 3–14; b) M. E. Davis, *Nature* **2002**, *417*, 813–821; c) N. Rosi, J. Eckert, M. Eddaoudi, D. Vodak, J. Kim, M. O′Keeffe, O. M. Yaghi, *Science* **2003**, *300*, 1127–1129; d) A. Corma, *Chem. Rev.* **1997**, *97*, 2373–2419; e) G. Férey, *Chem. Soc. Rev.* **2008**, *37*, 191–214; f) R. E. Morris, X. Bu, *Nat. Chem.* **2010**, *2*, 353–361; g) E. R. Cooper, C. D. Andrews, P. S. Wheatley, P. B. Webb, P. Wormald, R. E. Morris, *Nature* **2004**, *430*, 1012–1016.

[2] a) R. F. Lobo, M. Tsapatsis, C. C. Freyhardt, S. Khodabandeh, P. Wagner, C. Y. Chen, K. J. Balkus, Jr., S. I. Zones, M. E. Davis, *J. Am. Chem. Soc.* **1997**, *119*, 8474–8484; b) K. G. Strohmaier, D. E. W. Vaughan, *J. Am. Chem. Soc.* **2003**, *125*, 16035–16039; c) X. Zou, T. Conradsson, M. Klingstedt, M. S. Dadachov, M. O′Keeffe, *Nature* **2005**, *437*, 716–719; d) K. E. Christensen, C. Bonneau, M. Gustafsson, L. Shi, J. Sun, J. Grins, K. Jansson, I. Sbille, B. L. Su, X. Zou, *J. Am. Chem. Soc.* **2008**, *130*, 3758–3759; e) Y. Zhou, H. Zhu, Z. Chen, M. Chen, Y. Xu, H. Zhang, D. Zhao, *Angew. Chem. Int. Ed.* **2001**, *40*, 2166–2168; *Angew. Chem.* **2001**, *113*, 2224–2226; f) J. Sun, C. Bonneau, Á. Cantín, A. Corma, M. J. Díaz-Cabañas, M. Moliner, D. Zhang, M. Li, X. Zou, *Nature* **2009**, *458*, 1154–1158; g) M. Estermann, L. B. McCusker, C. Baerlocher, A. Merrouche, H. Kessler, *Nature* **1991**, *352*, 320–323; h) N. Guillou, Q. Gao, P. M. Forster, J. S. Chang, M. Noguès, S. E. Park, G. Férey, A. K. Cheetham, *Angew. Chem. Int. Ed.* **2001**, *40*, 2831–2834; *Angew. Chem.* **2001**, *113*, 2913–2916; i) Y. C. Chang, S. L. Wang, *J. Am. Chem. Soc.* **2012**, *134*, 9848–9851; j) P. C. Jhang, Y. C. Yang, Y. C. Lai, W. R. Liu, S. L. Wang, *Angew. Chem. Int. Ed.* **2009**, *48*, 742–745; *Angew. Chem.* **2009**, *121*, 756–759; k) H. L. Huang, S. L. Wang, *Chem. Commun.* **2010**, *46*, 6141–6143.

[3] a) Y. C. Yang, S. L. Wang, *J. Am. Chem. Soc.* **2008**, *130*, 1146–1147; b) Y. C. Liao, C. H. Lin, S. L. Wang, *J. Am. Chem. Soc.* **2005**, *127*, 9986–9987.

[4] a) H. Li, M. Eddaoudi, M. O′Keeffe, O. M. Yaghi, *Nature* **1999**, *402*, 276–279; b) M. Eddaoudi, J. Kim, N. Rosi, D. Vodak, J. Wachter, M. O′Keeffe, O. M. Yaghi, *Science* **2002**, *295*, 469–472.

[5] H. Y. Lin, C. Y. Chin, H. L. Huang, W. Y. Huang, M. J. Sie, L. H. Huang, Y. H. Lee, C. H. Lin, K. H. Lii, X. Bu, S. L. Wang, *Science* **2013**, *339*, 811–813.

[6] C. T. Kresge, M. E. Leonowicz, W. J. Roth, J. C. Vartuli, J. S. Beck, *Nature* **1992**, *359*, 710–712.

[7] J. Seok, D. Kim, S. Shin, D. Moon, S. J. Cho, M. S. Lah, *Chem. Mater.* **2014**, *26*, 1711–1719.

[8] M. E. Davis, *Acc. Chem. Res.* **1993**, *26*, 111–115.

[9] Y. H. Hu, L. Zhang, *Adv. Mater.* **2010**, *22*, E1–E14.

[10] a) C. H. Lin, Y. C. Yang, C. Y. Chen, S. L. Wang, *Chem. Mater.* **2006**, *18*, 2095–2101; b) P. C. Jhang, N. T. Chuang, S. L. Wang, *Angew. Chem. Int. Ed.* **2010**, *49*, 4200–4204; *Angew. Chem.* **2010**, *122*, 4296–4300.

[11] H. L. Huang, Y. C. Lai, Y. W. Chiang, S. L. Wang, *Inorg. Chem.* **2012**, *51*, 1986–1988.

[12] Crystal data for 14-α: $Zn_2PO_8N_2C_{15}H_{17}$, M = 515.06, monoclinic, space group $P2_1/c$ (no. 14), $a = 5.3408(1)$, $b = 34.585(1)$, $c = 10.8468(3)$ Å; $\beta = 108.435(2)°$, $V = 1900.73(8)$ Å^3, $Z = 4$; $D = 1.800$ g cm^{-3}, $R1 = 0.0871$, and $wR2 = 0.1933$. Crystal data for 14-β: $Zn_2PO_8N_2C_{15}H_{17}$, M = 515.06, triclinic, space group P-1 (no. 2), $a = 5.3502(4)$, $b = 10.4817(8)$, $c = 17.576(1)$ Å; $\alpha = 77.292(2)°$, $\beta = 88.012(2)°$, $\gamma = 78.766(2)°$, $V = 943.1(1)$ Å^3, $Z = 2$; $D = 1.814$ g cm^{-3}, $R1 = 0.0338$, and $wR2 = 0.0594$.

[13] L. Carlucci, G. Ciani, D. M. Proserpio, S. Rizzato, *CrystEngComm* **2002**, *4*, 121–129.

[14] M. D. Allendorf, C. A. Bauer, R. K. Bhakta, R. J. T. Houk, *Chem. Soc. Rev.* **2009**, *38*, 1330–1352.

[15] Y. C. Liao, F. L. Liao, W. K. Chang, S. L. Wang, *J. Am. Chem. Soc.* **2004**, *126*, 1320–1321.

[16] T. L. Malkin, A. Goddard, D. E. Heard, P. W. Seakins, *Atmos. Chem. Phys.* **2010**, *10*, 1441–1459.

[17] T. B. Faust, D. M. D′Alessandro, *RSC Adv.* **2014**, *4*, 17498–17512.

